https://doi.org/10.2352/CIC.2026.34.1.40
©2026 Society for Imaging Science and Technology

Color Vision Deficiency and Color Rendering Indices

Rafael Huertas; Department of Optics, Faculty of Science, University of Granada; Granada, Spain.
Antonio M. Pozo; Department of Optics, Faculty of Science, University of Granada; Granada, Spain.
Luis Gómez Robledo; Department of Optics, Faculty of Science, University of Granada; Granada, Spain.
Samuel Morillas; Instituto Universitario de Matemática Pura y Aplicada, Universidad Politécnica de Valencia; Valencia, Spain.
Michael J. Murdoch; Munsell Color Science Laboratory, Rochester Institute of Technology, Rochester, NY, USA.

Abstract

A Color Rendering Index (CRI) evaluates how accurately a light source replicates the colors of an object compared to a standard illuminant. Traditional lighting metrics, including the CIE R_a index, the Color Quality Scale with its Q_a index, and the ANSI/IES TM-30-20 method, rely on normal color vision models, neglecting the 8% of Caucasian men and 0.5% of Caucasian women affected by Color Vision Deficiency (CVD). This study aims to bridge this gap by studying rendering metrics for observers with CVD using algorithmic simulations that model various categories and severities of color vision impairment, with a dataset of 318 spectral power distributions (SPDs), comprising both theoretical illuminants and commercial lamps. CVD was simulated using the Lucassen et al. model to adjust L- and M-cone responses, modeling mild, medium, and severe protan and deutan conditions. Our results show a systematic increase in fidelity indices (R_a, Q_a, and R_f) as CVD severity increases, as a reduced color gamut means fewer spectral regions require accurate reproduction. However, Q_a and R_f demonstrated greater robustness than R_a in detecting underlying spectral deficiencies. The Gamut Index (R_g) served as the most effective index. Furthermore, standard deviations of fidelity indices decreased sharply with CVD severity, indicating highly homogeneous and predictable responses to spectral shifts among severe dichromats. These findings demonstrate that standard lighting metrics are not inclusive of the CVD population.

Introduction

To evaluate the performance of light sources, several key parameters are considered: luminous efficacy, correlated color temperature (CCT), and the Color Rendering Index (CRI). Among these, CRI is a vital metric in lighting design, as it quantifies how accurately a source replicates colors compared to a natural reference like daylight. Fundamentally, any rendering index serves as a numerical gauge of a light source's ability to reveal an object's "true" colors. Sources with a low CRI often result in dull or distorted hues, making high CRI lighting indispensable in environments where visual precision is paramount, including art and culture, healthcare, commerce, and media. Additionally, the aesthetic benefits of a good CRI are appreciated in homes and other environments.

The International Commission on Illumination (CIE) established the CIE R_a index as the global benchmark in 1995 [1]. This scale peaks at 100, a value reserved for sources with a spectrum matching daylight or a black-body radiator, such as incandescent bulbs, whereas traditional fluorescent lights vary wildly, ranging from approximately 50 for basic models to 98 for high-end multi-phosphor versions. In recent years, the lighting landscape has been transformed by the LED revolution. Unlike older technologies, LEDs allow for significant customization of their SPD. While standard white LEDs typically achieve an $R_a \geq 80$, the R_a metric itself has faced criticism. Critics argue that it fails to accurately predict color appearance in modern lighting, which has led to the development of more robust frameworks [2], [3].

A precise and robust method for comprehensively characterizing color rendition is critical to specifying appropriate light sources and optimizing their spectral characteristics. In 2010, Davis and Ohno at NIST introduced the Color Quality Scale (CQS) and its Q_a index [4]. CQS addresses the shortcomings of CRI by utilizing a broader set of color samples and evaluates aspects of color quality by accounting for factors like chroma and saturation, which significantly influence human perception. Q_a index is based on psychophysical experiments where observers rate the color quality of a light source using 15 distinct color samples.

In 2020, the Illuminating Engineering Society published an American National Standard method for evaluating source color rendition (ANSI/IES TM-30-20) [5], as an evolution of the IESNA TM-30-15, published in 2015. This Technical Memorandum presents a method for objectively and statistically characterizing the color rendition of light sources through the evaluation of 99 color samples. It evaluates both overall properties, such as color fidelity and gamut area, and hue-specific attributes, including fidelity, chroma shift, and hue shift, using numerical and graphical tools. This approach is not intended to represent human perception or preferences, nor to reduce color rendition to a single metric. Instead, it provides a set of complementary measures that users can interpret based on experience or application.

These methods are based on the average color difference between a set of samples illuminated by the test light source and a reference light source under the assumption of normal color vision. However, Color Vision Deficiency (CVD), is prevalent, affecting roughly 8% of Caucasian men and 0.5% of women [6]. The most frequent manifestations are protanopia/deuteranopia (red-green blindness caused by the absence or malfunction of L or M cones). Tritanopia is a much rarer blue-yellow deficiency involving S cones. CVD significantly complicates daily life, from interpreting traffic signals to judging food ripeness [7]. The last decade has seen a surge in assistive technologies designed to improve color discrimination for individuals with CVD. Because these individuals perceive colors differently, traditional CRI, CQS or TM-30-20 values do not accurately reflect their visual experience. Consequently, there is a growing need for lighting metrics that account for the type and intensity of these visual impairments. Such data could eventually be integrated into the commercial specifications of lighting products to better serve diverse populations.

This research aims to analyze how light source performance metrics shift when viewed by CVD observers, complementing our previous work [8]. By employing algorithmic simulations of various types and severities of color deficiency, we study CRI, CQS and TM-30-20 with the last objective of adapting them to be more inclusive of the diverse ways humans perceive colors.

Method

All computations were performed, through MATLAB, using spectral data from 380 to 780 nm in 2 nm increments for CRI and CQS and 1 nm for TM-30-20. If the data (spectral power distribution, spectral reflectance or Color Matching Functions) were not originally in that format, we employed derivative-constrained-spline interpolation. Extrapolation was never done.

Lamps and reference illuminants

For this study different light source (or lamp) SPDs have been obtained from the dataset provided, as Excel sheet, in the TM-30-20 calculation tools[5]. TM-30-20 includes a set of 318 SPDs which is a subset of SPDs used in [9]. From this dataset we are going to extract the following groups:

- Theoretical illuminants: the equal energy illuminant and the 12 CIE fluorescent illuminants (F1 to F12).
- Commercial lamps (Fig. 1): 17 commercial fluorescent broadband (Fig. 1a), 22 commercial fluorescent narrowband (Fig.1b), 20 commercial high intensity discharge (Fig. 1c), 8 commercial halogen (Fig. 1d), 4 commercial incandescent (Fig. 1e), 8 commercial LED hybrid (Fig. 1f), 1 commercial LED mixed (Fig. 1g) and 129 commercial LED phosphor (Fig. 1h).

The reference illuminants used to compute R_a and Q_s match those specified in [1], [4], i.e., for test sources with CCT < 5000 K, the reference illuminant is a Planckian radiator at the same CCT as the test source. For test sources at CCT ≥ 5000 K, the reference is a phase of the CIE Daylight illuminant having the same CCT as the test source, computed following the CIE recommendations [10]. For TM-30-20 a Planckian radiator is used for CCT ≤ 4000 K and a phase of the CIE Daylight illuminant for CCT ≥ 5000 K. In the case of 4000 < CCT < 5000 K the reference illuminant is a proportional mix of Planckian radiator and the CIE Daylight illuminant [5], overcoming the discontinuity at 5000 K of the previous methods.

CIE R_a

The R_a index is the CRI currently recommended by the CIE, computed according to [1]. It represents the average color difference of eight test samples under the test light source versus the reference light source. These color differences were determined using the CIE 1964 U*W*V* uniform color space after applying a von Kries-type chromatic adaptation. To calculate the individual indexes R_i for each sample, a normalization process was applied as follows:

$$R_i = 100 - 4.6\Delta E_i \tag{1}$$

Finally, R_a is computed as the average of the R_i values for the eight samples. Because of the normalization in Eq. (1) negative values of R_a are possible.

CQS Q_a

A set of 15 color samples was selected to encompass a broad gamut, including both saturated and unsaturated colors. Following the methodology proposed by Davis and Ohno [4], the CQS calculation resembles the CRI framework; however, it utilizes the CMCCAT2000 chromatic adaptation model, and color differences are calculated in the CIELAB color space ($\Delta E_{ab,i}$). Subsequently, a saturation factor is applied to counteract any contribution to the color difference from an increase in object chroma under test source illumination relative to the reference illuminant, obtaining ($\Delta E_{ab,i,sat}$). Evidence suggests that increases in object chroma, if not excessive, are not detrimental to color quality and may even be beneficial. To maintain neutrality, the saturation factor ensures that an increase in object chroma is neither penalized nor rewarded.

The color differences from all 15 samples are considered. If the color differences were merely combined by averaging all 15 color differences, then the Q_a score could be still relatively high even if one or two color samples show very large color differences. This situation is entirely possible with the notable peaks and valleys of RGB LEDs, which can render a couple of object colors poorly, while performing well for the rest. To ensure that poor rendering of even a few object colors has a significant impact on the General Color Quality Scale, the color differences are combined using the root mean square (ΔE_{rms}).

Afterwards, a scaling factor is introduced to obtain ($Q_{a,rms}$):

$$Q_{a,rms} = 100 - 3.1\Delta E_{rms} \tag{2}$$

To prevent negative values (as can happens in R_a), the final scores are converted to a 0–100 scale ($Q_{a,0\text{-}100}$) by:

$$Q_{a,0-100} = 10\ln\left(e^{\frac{Q_{a,rms}}{10}} + 1\right) \tag{3}$$

A final CCT factor (M_{CCT}) is devised to penalize light sources with extremely low CCTs, which have smaller gamut areas and, therefore, exhibit decreased chromatic discrimination performance. The general CQS is calculated as follows:

$$Q_a = M_{CCT} Q_{a,0-100} \tag{4}$$

TM-30-20

The TM-30-20 method [5] provides a multidimensional approach with multiple layers of objective information. Among others, in this work we consider the Fidelity Index (R_f), which is bounded at 100, and the Gamut Index (R_g), which measures whether the light source, on average, saturates (above 100) or desaturates (below 100) colors compared to the reference.

This method expands the number of samples to 99 color evaluation samples (CES), which have been extracted from a dataset of more than 100,000, to quantify the difference in color rendition between the test source and reference illuminant. The Chromatic Adaptation Transformation applied is the one in the Color Appearance Model CAM02. The color difference is computed following the CAM02-UCS formula in the *J'a'b'* space ($\Delta E_{jab,i}$) [11].

The Fidelity Index (R_f) evaluates the average similarity of 99 color samples compared to a reference illuminant on a scale from 0 to 100 and is computed as follows:

$$R'_f = 100 - 6.73\left[\frac{1}{99}\sum_{i=1}^{99}\left(\Delta E_{jab,i}\right)\right] \tag{5}$$

Finally, to avoid negative values the scale is adjusted by the same logarithmic function than Eq. 3, substituting $Q_{a,rms}$ by R'_f.

The Gamut Index (R_g) is calculated as 100 times the ratio of the area (in the CAM02 a',b' space) of the two polygons, computed for the samples illuminated with the test and reference lights respectively. It measures the average change in saturation (chroma) or color gamut area caused by the light source. Values near 100 indicate a gamut area similar to the reference; values above 100 indicate oversaturation, and values below 100 indicate undersaturation, relative to the reference illuminant.

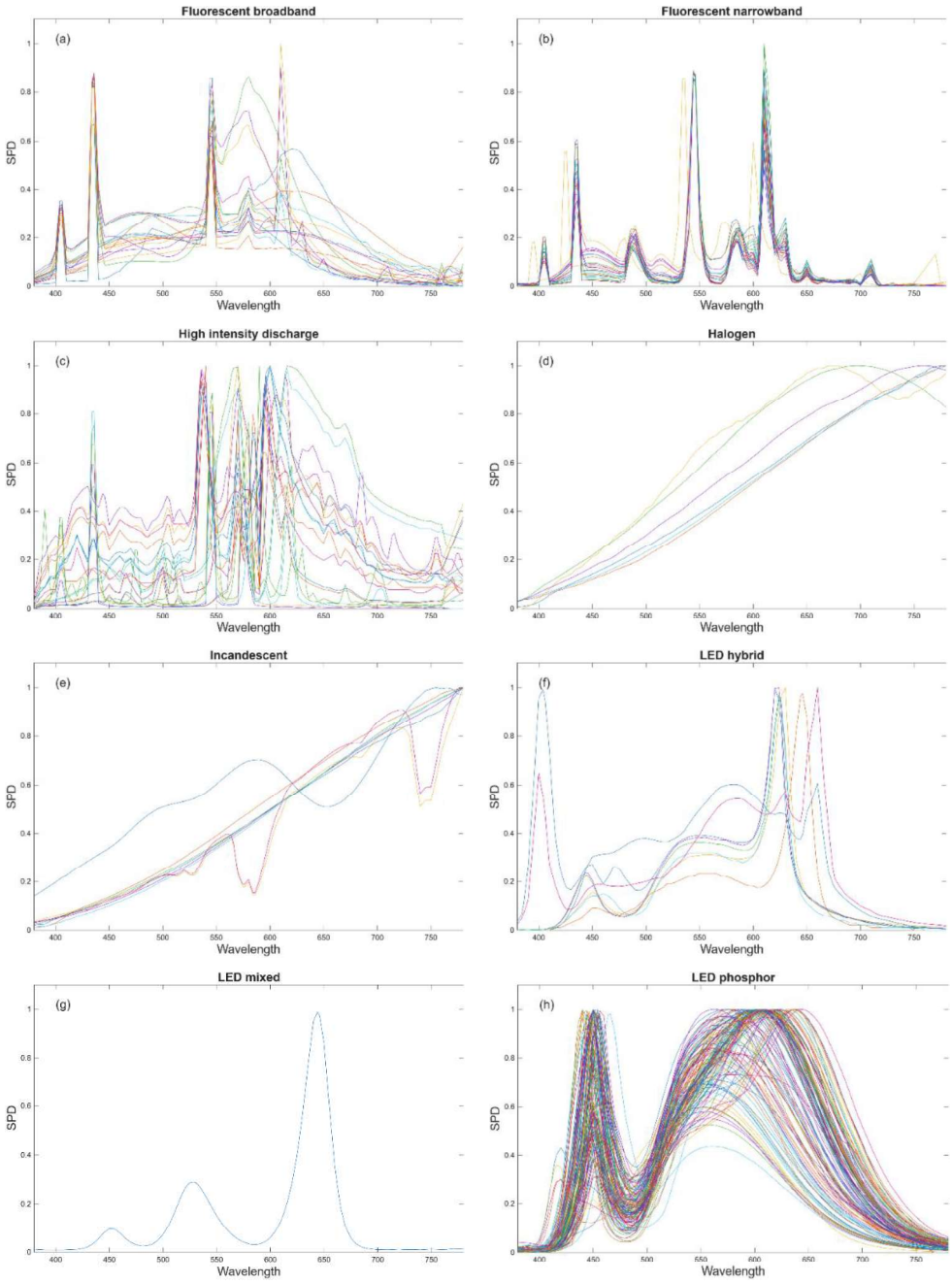

Figure 1. SPDs of the light sources in the 8 groups considered.

Simulation of anomalous color vision

The aforementioned indices (R_a, Q_a, R_f and R_g) were first computed for normal color vision observers, following the proposed equations. Additionally, they have been computed for color vision deficient (CVD) observers using the model proposed by Lucassen et al. [12]. This model adjusts L- and M-cone responses in anomalous observers by applying a weighting parameter, d.

In the computations of these indices, tristimulus values of a set of samples are computed under the test illuminant and a reference illuminant. In this point a transformation from XYZ and to LMS has been done by Golz and MacLeod [13] to apply the CVD model. A value of $d = 0$ represents normal color vision, $d = 1$ indicates protanopia or deuteranopia, and intermediate values represent varying severities of protanomaly or deuteranomaly. For both protan and deutan types, three distinct conditions were modeled by considering $d = 0.3$ and $d = 0.6$, which represent mild and medium severities, respectively, based on thresholds established in prior studies. For each case, the obtained LMS values are transformed back into XYZ, which are then fed back into the calculation of the indices, using the same color models as for normal color vision.

Results and discussion

Accounting for CVD, via the Lucassen algorithm, modifies the indices significantly, as detailed in Tables 1-4. In these tables, the groups of lamps are designed as follow: Equal energy (EE), CIE fluorescent illuminants (CIE F), Fluorescent broadband (FB), Fluorescent narrowband (FN), High intensity discharge (HID), Halogen (H), Incandescent (I), LED hybrid (LEDH), LED mixed (LEDM), and LED phosphor (LEDP). Except for EE and LEDH, with only one lamp, all data represents the mean values with the standard deviation reported in parentheses.

Table 1: R_a values (average if case) for different CVD conditions and the groups of lamps. Standard deviation is shown in parentheses where applicable.

	EE	CIE F	FB	FN	HID
Normal	95.28	75.24 (14.57)	80.97 (14.99)	81.54 (4.36)	67.35 (28.92)
Mild protan.	96.06	81.16 (10.82)	85.36 (11.14)	85.33 (3.18)	74.40 (22.90)
Med. protan.	96.24	86.91 (6.87)	89.30 (7.03)	88.69 (2.06)	81.50 (16.29)
Protan.	94.90	92.00 (2.99)	92.23 (3.37)	90.84 (1.63)	88.39 (11.11)
Mild deuter.	96.88	81.58 (10.27)	85.51 (10.70)	85.62 (3.10)	76.38 (21.01)
Med. deuter.	96.91	87.07 (6.57)	89.23 (7.01)	89.19 (2.22)	83.83 (15.16)
Deuter.	95.83	91.36 (3.88)	91.51 (4.17)	91.88 (1.99)	88.71 (12.16)
	H	I	LEDH	LEDM	LEDP
Normal	98.74 (1.71)	92.67 (10.31)	89.56 (5.15)	23.86	79.41 (7.52)
Mild protan.	98.89 (1.49)	94.48 (7.76)	91.72 (3.78)	42.32	84.11 (5.82)
Med. protan.	99.02 (1.29)	96.50 (4.80)	93.94 (2.46)	63.16	88.64 (4.32)
Protan.	98.95 (1.35)	98.07 (2.34)	96.12 (1.43)	87.89	92.55 (3.39)
Mild deuter.	98.99 (1.33)	95.13 (6.81)	92.26 (3.48)	49.02	84.67 (5.93)
Med. deuter.	99.09 (1.21)	96.99 (4.05)	94.58 (2.09)	70.76	89.19 (4.60)
Deuter.	99.04 (1.24)	98.15 (2.25)	96.42 (1.31)	90.46	92.61 (3.57)

Table 1 presents the R_a values calculated for the selected light sources across different observer categories: normal color vision, protanomalous (mild and medium), protanope, deuteranomalous (mild and medium), and deuteranope. Tables 2 to 4 do the same for the indexes Q_a, R_f and R_g respectively.

The data in Table 1 reveal a systematic increase in R_a values as the severity of CVD increases. This phenomenon occurs because individuals with CVD possess a reduced color gamut; consequently, fewer spectral regions require accurate reproduction to satisfy their visual system. Thus, across all lamp categories, normal color vision observers yield the lowest R_a values, whereas protanopes exhibit the highest. The highest R_a values in Table 1 correspond to the halogen lamps (Fig. 1d), whereas the lowest values are observed for the mixed LED source (Fig. 1g). For LEDs, the most significant shift occurs in the mixed LED (LEDM) sources (Fig. 1g), jumping from a poor 23.86 for normal color vision to 87.89 for a protanope and 90.46 for a deuteranope. This suggests that the spectral distributions of these sources, while problematic for normal color vision, are largely imperceptible to those with red-green deficiencies. Furthermore, the standard deviation within lamp groups decreases in CVD cases, indicating that different lamps within a category appear more uniform in color reproduction to CVD observers than to normal ones

Table 2: Q_a values (average if case) for different CVD conditions and the groups of lamps. Standard deviation is shown in parentheses where applicable.

	EE	CIE F	FB	FN	HID
Normal	83.87	75.64 (12.46)	78.02 (13.32)	78.80 (6.14)	64.57 (26.14)
Mild protan.	86.20	80.79 (10.05)	82.16 (10.71)	82.98 (5.38)	70.16 (20.86)
Med. protan.	88.38	85.84 (7.48)	86.34 (8.09)	86.87 (4.59)	76.17 (16.02)
Protan.	90.89	92.34 (3.47)	91.95 (4.92)	91.52 (3.56)	85.47 (10.48)
Mild deuter.	86.51	81.72 (9.35)	82.78 (10.14)	83.37 (5.26)	71.37 (20.40)
Med. deuter.	89.63	86.68 (6.93)	86.60 (7.62)	87.25 (4.75)	76.87 (15.65)
Deuter.	93.19	89.31 (5.81)	88.39 (6.31)	89.73 (4.47)	79.55 (14.08)
	H	I	LEDH	LEDM	LEDP
Normal	91.52 (9.01)	89.39 (9.73)	85.63 (5.42)	58.82	78.06 (6.91)
Mild protan.	91.71 (8.75)	89.76 (9.33)	86.96 (5.62)	60.16	82.23 (5.66)
Med. protan.	92.00 (8.33)	90.17 (8.93)	88.48 (5.96)	61.43	86.53 (4.80)
Protan.	92.76 (7.32)	90.91 (8.19)	90.77 (6.55)	63.04	92.79 (4.12)
Mild deuter.	92.00 (8.31)	90.13 (8.92)	87.52 (5.37)	65.54	82.93 (5.51)
Med. deuter.	92.54 (7.52)	90.90 (8.14)	89.17 (5.38)	72.59	87.01 (4.68)
Deuter.	93.06 (6.86)	91.74 (7.33)	90.57 (5.50)	78.55	89.74 (4.48)

Table 2 shows a relative stability of Q_a against R_a. While Q_a also increases with CVD severity, it demonstrates greater robustness than R_a. For instance, the LEDM source (Fig. 1g), which exhibited a massive 64-point jump in R_a, only increases from 58.82 (normal color vision) to 63.04 for protanopia in Q_a. This smaller increase suggests that the CQS metric is better at identifying underlying quality issues in the lamps that persist even when the observer's color discrimination is impaired.

The Q_a index remains lower than R_a under poor spectral conditions (i.e. HID lamps: 64.57 Q_a vs. 67.35 R_a for normal vision), proving to be a stricter indicator of human color dissatisfaction.

Similarly, Table 3 shows that the Fidelity Index (R_f) rises as discrimination capacity decreases. However, R_f systematically yields lower scores and punishes spectral gaps more severely than the traditional R_a (Table 1) for normal and mild observers. Evaluating 99 color patches instead of 8 effectively eliminates the "lucky match" phenomenon where discontinuous peak-spectrum sources trick the older R_a metric. The most important shifts in R_f happen for the phosphor LED (LEDP) group (Fig. 1h), where the

index increases from 79.97 (normal color vision) to 87.29 (protanope) and 88.65 (deuteranope). These results confirm that for the CVD population the requirements for the spectral power distribution are less restrictive than for normal color vision observers.

Table 3: R_f values (average if case) for different CVD conditions and the groups of lamps. Standard deviation is shown in parentheses where applicable.

	EE	CIE F	FB	FN	HID
Normal	94.71	77.57 (11.79)	82.09 (11.56)	78.99 (4.04)	68.46 (23.25)
Mild protan.	94.77	80.50 (10.28)	84.34 (9.90)	81.35 (3.67)	72.21 (19.72)
Med. protan.	95.03	83.68 (8.54)	86.77 (7.99)	83.78 (3.32)	76.44 (15.66)
Protan.	95.76	87.52 (6.33)	89.78 (5.72)	86.28 (2.99)	81.47 (11.01)
Mild deuter.	95.22	81.24 (9.52)	84.77 (9.20)	81.79 (3.50)	74.24 (18.52)
Med. deuter.	95.60	84.74 (7.52)	87.32 (7.08)	84.44 (3.11)	79.22 (14.59)
Deuter.	96.12	87.29 (6.45)	89.16 (5.83)	86.73 (3.19)	82.42 (12.43)
	H	I	LEDH	LEDM	LEDP
Normal	98.50 (1.51)	95.59 (5.69)	88.79 (2.05)	57.95	79.97 (6.52)
Mild protan.	98.52 (1.51)	96.01 (5.10)	89.85 (1.98)	61.61	82.26 (5.54)
Med. protan.	98.56 (1.47)	96.58 (4.31)	91.04 (1.97)	66.12	84.65 (4.62)
Protan.	98.66 (1.35)	97.65 (2.85)	92.59 (2.05)	73.32	87.29 (3.81)
Mild deuter.	98.60 (1.39)	96.46 (4.47)	90.37 (1.95)	66.10	82.98 (5.49)
Med. deuter.	98.67 (1.32)	97.18 (3.44)	91.74 (1.97)	74.12	86.08 (4.44)
Deuter.	98.75 (1.22)	97.66 (2.76)	92.68 (1.99)	81.69	88.65 (3.59)

The gamut index, R_g, of ANSI/IES TM-30-20 (Table 4), provides the most critical insight into the real-world visual experience of CVD individuals. In protanopia, R_g values drop significantly across nearly all sources. The mixed LED (LEDM) source (Fig. 1g) falls from a highly saturated 116.67 (normal color vision) to 89.17 (protanope). This indicates that colors appearing vibrant to normal observers are perceived as severely desaturated or "muddy" by protanopes. In comparison across the lamps, protanopes experience the best gamut with fluorescents and high intensity discharge sources. Interestingly, for deuteranopia, many R_g values increase above 100. For example, Narrowband Fluorescent (FN) lamps increase from 100.1 to 105.9. This suggests that certain light sources may enhance the sensation of saturation for deutan observers, potentially aiding color discrimination.

A global analysis of the indices shows that in pure fidelity indices (R_a, Q_a, R_f), a compelling mathematical pattern emerges. As the severity of CVD increases from mild to medium, and finally to severe dichromats (protan/deutan), the standard deviations (values in parentheses) decrease sharply. This indicates that severe observers experience a much more homogeneous, narrow, and predictable response to spectral shifts than normal or mild observers. Although it is not the largest group, HID lamps exhibit the highest standard deviation values across all indices, due to their discontinuous spectral nature.

Differences between protan (L-cone affected) and deutan (M-cone affected) subjects become significantly more pronounced under narrow-band or multi-peak light sources, such as LEDs and HID lamps. This is tied to the critical positioning of the spectral sensitivity peaks of these photoreceptors. Because the spectrum is filled with deep "valleys" and sharp "peaks", any minor variation in the cone sensitivity curves causes the light to be perceived radically differently. This proves that HID sources provide highly unpredictable and unreliable color rendering for universal lighting design, as the color experience varies extremely among individuals.

Table 4: R_g values (average if case) for different CVD conditions and the groups of lamps. Standard deviation is shown in parentheses where applicable.

	EE	CIE F	FB	FN	HID
Normal	102.7	93.09 (7.51)	96.20 (7.00)	100.1 (2.33)	90.14 (13.57)
Mild protan.	100.5	93.52 (4.56)	94.82 (5.27)	98.54 (1.99)	90.89 (11.23)
Med. protan.	99.43	95.70 (3.13)	96.15 (3.51)	99.55 (1.99)	90.64 (7.76)
Protan.	90.44	93.51 (1.03)	93.40 (0.96)	93.45 (0.69)	93.08 (2.18)
Mild deuter.	101.9	98.49 (4.33)	98.86 (4.62)	99.43 (1.91)	93.00 (9.93)
Med. deuter.	100.02	96.21 (3.73)	96.41 (3.50)	98.33 (1.43)	94.28 (6.74)
Deuter.	104.1	105.6 (0.38)	105.5 (0.39)	105.9 (0.28)	105.70 (0.92)
	H	I	LEDH	LEDM	LEDP
Normal	98.14 (0.89)	99.90 (3.78)	98.51 (2.87)	116.67	94.78 (2.62)
Mild protan.	97.98 (1.24)	99.14 (3.60)	98.60 (2.84)	114.51	95.40 (2.33)
Med. protan.	94.84 (1.39)	95.56 (2.62)	96.24 (2.80)	108.13	93.91 (1.95)
Protan.	90.10 (0.20)	90.11 (0.07)	91.06 (0.83)	89.17	91.47 (1.14)
Mild deuter.	95.05 (0.60)	97.40 (2.66)	98.82 (3.00)	113.50	95.54 (2.28)
Med. deuter.	90.74 (0.50)	92.16 (1.49)	94.32 (2.34)	103.58	96.63 (1.58)
Deuter.	105.26 (0.22)	105.35 (0.19)	104.83 (0.81)	104.03	104.24 (0.27)

Equal Energy (EE) and Halogen (H) sources maintain the highest and most stable values across all fidelity indices (R_a, Q_a, and $R_f \approx$ 90%-99%). For the gamut index (R_g), Halogen lamps stay remarkably close to 100 for normal observers (98.14), dropping only slightly for severe protanopes (90.10). In the case of LED.

In the case of LEDM (multi-chip or RGB LED) lamps, normal observers experience terribly low fidelity (Q_a=58.82, R_f=57.95) but a heavily oversaturated gamut (R_g=116.67). However, as CVD severity increases, the fidelity indices paradoxically increase (e.g., R_a rises from 23.86 to 87.89 for protanopes). This proves that RGB-mixed LEDs generate massive saturation distortions that severe CVD individuals perceive radically differently due to overlapping spectral curves, registering a false mathematical increase in fidelity.

Furthermore, the oversaturation experienced by a normal observer (R_g=116.67) completely collapses for a protanope (R_g=89.17), shifting to severe undersaturation and a loss of color gamut area. Conversely, LEDP (phosphor-converted LED) sources show a much more stable, intermediate performance (R_a, $R_f \approx$ 80%-92%) across all observer types, making them a far more reliable and safer choice for universal, inclusive lighting design

High-Intensity Discharge Lamps exhibit the worst overall color rendition performance and the widest standard deviations (frequently exceeding ±15 to ±25). Because their emission spectrum consists of discrete, discontinuous gas lines, color rendering predictability for CVD observers under HID lighting is highly volatile and poor.

Conclusion

These results are based on the hypothesis that chromatic adaptations, color differences and/or appearance descriptors can be just applied for CVD observers after the transformation in LMS space, the validity of which is arguable. Anyway, assuming this hypothesis, the analysis demonstrates that standard lighting metrics (R_a, Q_a, R_f) are not inclusive of the approximately 8% of the male population with color vision deficiencies. These fidelity-based indices are inflated when computed for CVD observers, suggesting high quality but ignoring the colors these individuals cannot discriminate, questioning the reference significance of these index scores. Sharp emission peaks characteristic of mixed LED and high intensity discharge lamps affect color-deficient individuals negatively and disrupt the reliability of traditional metrics. Modern frameworks like TM-30-20 offer a more accurate representation of color performance for accessible and inclusive lighting environments. The perceived volume of the color space changes dramatically depending on the specific photoreceptor deficiency, meaning fidelity alone is insufficient to describe CVD color perception. The Gamut Index (R_g) serves as the most effective differentiator, revealing a stark divergence in visual experience: while protans suffer from massive perceived desaturation, deutans may experience a saturation boost under certain sources. To serve a diverse population, lighting manufacturers and specifiers should move beyond average fidelity and consider these shifts to provide more inclusive and effective lighting solutions for all users. It would be desirable to carry out experimental work in future studies.

References

[1] Commission Internationale de l'Eclairage (CIE), "Method of measuring and specifying colour rendering properties of light sources," CIE Central Bureau, Vienna, Austria, Tech. Rep. CIE 13.3, 1995.

[2] Y. Ohno, "Spectral design considerations for white LED color rendering," Opt. Eng., vol. 44, (11), pp. 111302–9, 2005.

[3] Commission Internationale de l'Eclairage (CIE), "Colour rendering of white LED light sources," CIE Central Bureau, Vienna, Austria, Tech. Rep. CIE 177, 2007.

[4] W. Davis and Y. Ohno, "Color quality scale," Optical Engineering, vol. 49, (3), pp. 033602–16, 2010.

[5] ANSI/IES TM-30-20, "Technical memorandum: IES method for evaluating light source color rendition," Illumination Engineering Society, New York, NY, USA, 23 September. 2019.

[6] J. Birch, "Worldwide prevalence of red-green color deficiency," J. Opt. Soc. Am. A, vol. 29, (3), pp. 313–320, 2012.

[7] J. M. Steward and B. L. Cole, "What do color vision defectives say about everyday tasks?" Optometry Vision Sci., vol. 66, (5), pp. 288–295, 1989.

[8] R. Huertas et al, "Color Rendering Indexes for Color Blind Observers," in Proceedings of the 15th Congress of the International Colour Association 2023, Chiang Rai, Thailand, pp. 323–328, 2023.

[9] K. W. Houser et al, "Review of measures for light-source color rendition and considerations for a two-measure system for characterizing color rendition," Opt. Express., vol. 21, (8), pp. 10393–10411, 2013.

[10] Commission Internationale de l'Eclairage (CIE), "Colorimetry," CIE Central Bureau, Vienna, Austria, Tech. Rep. CIE 015, 2018.

[11] M. R. Luo, G. Cui and C. Li, "Uniform colour spaces based on CIECAM02 colour appearance model," Color Res. Appl., vol. 31, (4), pp. 320–330, 2006.

[12] M. P. Lucassen and J. W. Alferdinck, "Dynamic simulation of color blindness for studying color vision requirements in practice," in Third European Conference on Colour in Graphics, Imaging and Vision, Leeds, UK, 2006, pp. 37–41.

[13] J. Golz and D. I. MacLeod, "Colorimetry for CRT displays," J. Opt. Soc. Am. A, vol. 20, (5), pp. 769–781, 2003.

Authors Biography

Rafael Huertas received his BS in Physics (1997) and in Optics and Optometry (1998) from the Universidad de Granada, Spain, where he also earned his PhD in Physics (2004). Since 2011, he has been an Associate Professor in the Optics Department at the same university and has served as Head of the Department since 2021. His research interests focus on colorimetry, image color, color-difference formulas, and color spaces.

Antonio M. Pozo received his PhD from the Universidad de Granada (2008), where he has since served as an Associate Professor in the Optics Department. His research focuses on methods to evaluate the image quality of CCD and CMOS cameras, and the optical characterization of displays.

Luis Gómez Robledo received his PhD in optics from the Universidad de Granada (2010), where he has worked as an Assistant Professor in the Optics Department since 2018. His research focuses on color differences and color vision deficiencies.

Samuel Morillas holds a BSc in Computer Science from the Universidad de Granada and a PhD in Applied Mathematics from the Universitat Politècnica de València (UPV), Spain. Since 2019, he has been a full professor in the Applied Math Department at UPV and a member of the Institute of Pure and Applied Mathematics. His research focuses on fuzzy logic and fuzzy metrics, primarily their applications in image processing, color science, and pavement engineering.

Michael J. Murdoch is a Professor and Director of the Munsell Color Science Laboratory at the Rochester Institute of Technology. His academic research focuses on color appearance in augmented reality (AR) as well as color perception in displays and temporally dynamic LED lighting. He holds a BS in Chemical Engineering from Cornell, MS in Computer Science from RIT, and PhD in Human-Technology Interaction from Eindhoven University of Technology.